Northumbria Research Link

Energy distribution function based universal adsorption isotherm model for all types of isotherm

Muhammad Burhan*, Muhammad Wakil Shahzad and Kim Choon Ng

Water Desalination and Reuse Center (WDRC), Biological and Environmental Science & Engineering (BESE), King Abdullah University of Science and Technology (KAUST), Thuwal 23955-6900, Saudi Arabia

Abstract

Based upon the adsorbate–adsorbent interactions due to pore size distribution and surface heterogeneity, as characterized by the adsorption isotherms, the adsorption phenomenon has many industrial and environmental applications. These adsorption isotherms are very important to define the information related to the equilibrium uptake of adsorbate–adsorbent pair. Due to the presence of different energy distribution of adsorption sites, pore size distribution, surface area availability and surface heterogeneity, of each of the adsorbent–adsorbate pair, these isotherms are categorized into six types by the International Union of Pure and Applied Chemistry and so far, in the literature, there is no generalized adsorption isotherm model available that can define and predict the behavior of all adsorption isotherm types. In this study, a universal adsorption isotherm model is developed based upon the energy distribution function of the available adsorption sites and the pore size. The proposed model is able to define all adsorption isotherm characteristics, irrespective of their multi- or monolayer formations and micro- or meso-pore distribution.

*Corresponding author:
muhammad.burhan@kaust.
edu.sa

1 INTRODUCTION

Adsorption, of gas molecules onto a porous surface, is a very important phenomenon related to transformation and transport processes in the environment. Removal of toxics from air, especially in current environmental issues [1–6], wastewater treatment, purification of potable water, desalination of seawater [7–9] and gas storage [10–12]; adsorption process [13] has many industrial and environmental applications [14], based upon the adsorbate–adsorbent interaction. In physical adsorption, the adsorbate molecules are accommodated in mono- or multilayer formations, on the surface of the porous adsorbent by providing them a favorable energy state. The porous structure of adsorbents differs in terms of pore size, i.e. macropores, micropores and mesopores [15], causing different levels of surface heterogeneity and energy sites distribution for each pore size distribution (Figure 1). These pore size distribution and surface heterogeneity cause a unique interaction of each adsorbate–adsorbent pair, characterized by adsorption isotherms. The adsorption isotherms provide all information needed to study the adsorption equilibrium of adsorbate–adsorbent pair, while the adsorption model is the theory of the adsorption equilibrium. The International Union of Pure and Applied Chemistry (IUPAC) has categorized adsorption isotherms in six types, based upon the isotherm shape of adsorbate–adsorbent pairs. However, so far there is no universal adsorption model that can describe and fit the adsorption isotherms of all six types.

In literature, extensive work has been done for adsorption isotherm modeling. The isotherm models which are usable in the Henry's region, i.e. Henry, Tóth and Langmuir equations [16–18], do not remain valid in the high pressure range. Tóth proposed an isotherm model as the power function of the relation between adsorption potential of adsorbent surface and the adsorption uptake. Jaroniec and Marczewski's model [19–22] also followed Tóth concept of using power function [23]. However, later Tóth model was found to be limited as it failed to explain the isotherm transition from Henry to saturation region. Similarly, the isotherms models performing well in the
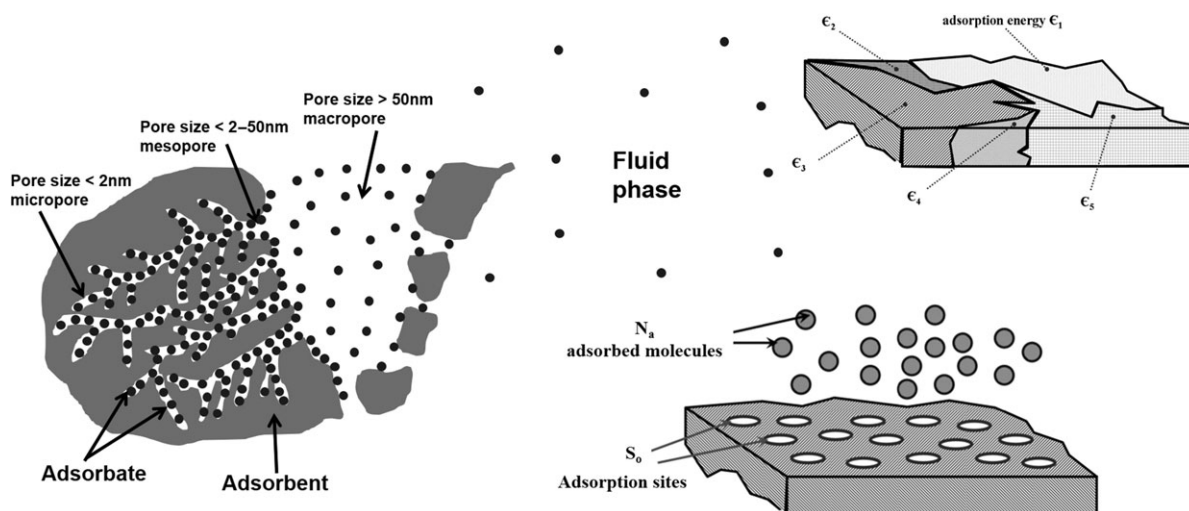
Figure 1. *Adsorption on complex heterogeneous porous surface.*

high pressure range near saturation, i.e. DA, and Dubinin and Radushkievich (DR) equation, fail to be consistent with low pressure experimental data [24–27]. Chakraborty and Sun proposed a modified Langmuir model, formulated in terms of Fermi–Dirac distribution [28]. Although, the proposed model showed significant consistency with Type-I, Type-II, Type-III and Type-V isotherms, but unable to describe the Type-IV. Khalfaousi *et al.* proposed separate analytical models for each of the five isotherms, in form of the modified Brunauer–Emmett–Teller isotherm model [29] using grand canonical ensemble. However, he also could not propose a universal model and theory describing all isotherm types.

Ross and Olivier proposed the theory of homotattic patch approximation [30] to divide the heterogeneous surface of adsorbent into small homogeneous patches, with known energy distribution function of adsorption energy sites. Frendlich [31], Sips [32, 33], Fowler [34] and Jovanovich [35] models also followed homotattic patch approximation and showed great agreement with most of the isotherm types, but none of the studies [36–38] able to unify the theory to model all types of adsorption isotherm. For the first time, in this paper, a universal adsorption model is proposed based upon the theory of localized adsorption, by also utilizing the homotattic patch approximation, in monolayer formation and its extension to multilayer formation, but with probability or fraction term of total surface coverage by stronger sites and heterogeneity factor, to predict all isotherms. The localized adsorption is defined as a function of energy distribution of adsorption sites.

2 UNIVERSAL ADSORPTION ISOTHERM MODEL

The proposed theory behind the developed universal adsorption isotherm model is based upon the homotattic patch approximation

as a function of the energy distribution of the adsorption sites, with monolayer coverage, which is then further proposed to be the fraction of the overall surface coverage among different pore sizes or multi-layers formation. As per the approximation, the heterogeneous surface of adsorbent is considered as the agglomeration of multiple homogeneous patches. Each homogeneous patch consists of multiple adsorption sites of same energy level and the size of homogeneous patches is defined in terms of the energy distribution function of the adsorption energy sites. Higher the probability of an adsorption site defines the higher localized adsorption uptake in monolayer coverage. However, this energy distribution function varies for different pore size categories, i.e. micropore and macro- or mesopores, and also for the multilayer formation. Therefore, a probability factor is introduced to define the fraction of the total surface coverage or the energy distribution, associated with each pore size or adsorbate layer, i.e. in case of multilayer formations.

If $\theta(\varepsilon)$ is the localized adsorption uptake of the homogeneous patch, as function of the adsorption energy site 'ε', and $X(\varepsilon)$ denotes the distribution function of the energy sites 'ε', then the total adsorption uptake of heterogeneous surface with homotattic patch approximation, is given by integral equation (1).

$$\theta_t = \int_0^\infty (\theta(\varepsilon) \times X(\varepsilon)) d\varepsilon \tag{1}$$

The ratio of the local available adsorption sites 's_i' to the total available adsorption sites 'S_o' is proportional to the energy distribution function $X(\varepsilon)$, and the maximum value of this ratio will be equal to unity over the entire adsorption surface.

$$\frac{s_i}{S_o}(\varepsilon) = X(\varepsilon) d\varepsilon \tag{2}$$

However, from Langmuir isotherm model and Condensation Approximation.

$$\lim_{T \to 0} \theta(\varepsilon) = \theta_c(\varepsilon) = \begin{cases} 0 & \text{for } \Delta\varepsilon \leq \varepsilon_c \\ 1 & \text{for } \Delta\varepsilon \geq \varepsilon_c \end{cases} \tag{3}$$

Therefore, the equation (1) becomes

$$\theta_t = \int_{\varepsilon_c}^{\infty} X(\varepsilon)\, d\varepsilon \tag{4}$$

The symmetrical Guassian function is approximated to represent the distribution of the homogeneous adsorption energy sites over the heterogeneous. Then, by solving the integral of equation (4), we can get the universal adsorption isotherm model as:

$$\theta_t = \sum_{i=1}^{n} \alpha_i \left\{ \frac{\left(\frac{p}{p_s}\exp\left(\frac{\varepsilon_o}{RT}\right)\right)^{\frac{RT}{m}}}{1 + \left(\frac{p}{p_s}\exp\left(\frac{\varepsilon_o}{RT}\right)\right)^{\frac{RT}{m}}} \right\}_i \tag{5}$$

where p_s represents the saturation pressure at the maximum possible uptake by an adsorbent. While p and T represent the adsorption pressure and temperature, respectively. However, R is the general gas constant. Rest of the parameters are fitted with the adsorption isotherm experimental data as discussed in following Section.

3 RESULTS AND DISCUSSION

In order to demonstrate the applicability of the proposed universal adsorption isotherm model, the behavior of all types of the IUPAC isotherms is simulated using universal adsorption isotherm model. By using the obtained values of the adsorption energy sites and their corresponding probability, the experimental isotherm data of all six types, obtained from the literature, is accurately simulated from the proposed model. Detailed discussion regarding the use of universal adsorption isotherm model to predict the isotherm behavior and corresponding adsorption energy site distribution, is presented below for each isotherm type.

3.1 Type-I
Figure 2 shows the experimental data for Silica Gel 3A and water [39], adsorbent–adsorbate pair isotherms obtained at different temperature and pressure conditions, characterized as Type-I isotherms. The adsorption isotherm data is fitted using proposed universal adsorption isotherm model. The blue line represents the data obtained from the universal adsorption isotherm model and the circular dots represents the experimental data points.

From the isotherm results, if looked closely, it can be seen that there is a small saturation step of adsorption uptake at the lower concentration. After that, there is a rapid and major increase in the adsorption uptake until the saturation limit. This shows that instead of single group of adsorption sites, as
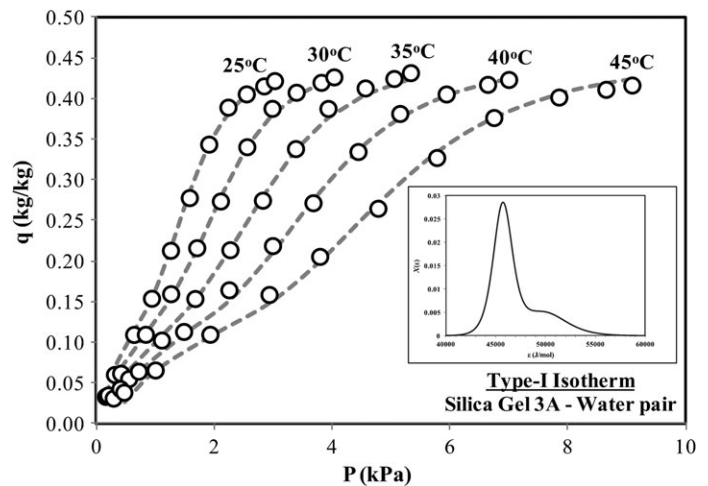

Figure 2. *Type-I adsorption isotherms experimental and prediction data.*

recommended by Langmuir model for Type-I isotherm, there are two different levels of adsorption sites. One of them is responsible for a small adsorption uptake at the lower concentration. However, the other is responsible for the major uptake, at higher concentration. In order to understand it further, the energy distribution graph for the adsorption sites, using energy distribution function and the regressed parameters, is plotted along with the adsorption uptake and shown in Figure 2. As depicted, two peaks represent the two levels of adsorption energy sites availability.

3.2 Type-II
Unlike Type-I isotherm, there is no horizontal saturation trend observed for Type-II isotherm. However, a rapid increase in the uptake can be seen when the relative pressure approaches unity. However, at lower pressure value, it exhibits similar trend of monolayer formation, like Type-I isotherm, reaching to intermediate saturation of adsorption surface. These two different trends are because of different pore size availabilities across the adsorption surface. The experimental data for Type-II isotherm for poorly crystalline boehmite and water adsorbent–adsorbate pair, obtained from [40] is shown in Figure 3. The experimental isotherm data is regressed using proposed universal adsorption isotherm model with two terms representing two different pore size groups as shown by the blue line in Figure 3. A perfect match experimental data and its trend is obtained by the proposed model.

The energy distribution graph shows two peaks, one with smaller value but larger width at higher energy value sites, and the other one with higher peak value but smaller width at lower energy value sites. At low concentration/pressure value, the adsorption uptake starts after crossing the probability peak for higher energy sites. However, it starts to flatten with drop in the energy distribution probability. This represents the first half of the adsorption uptake, that is similar to the Type-I isotherm.

However, at higher pressure/concentration, the second pore size group of low adsorption energy sites become available and after crossing the peak probability energy site, a rapid rise in the adsorption uptake can be seen, until the relative pressure becomes unity.

3.3 Type-III

The Type-III isotherm propagates similar to the Type-II isotherm. However, it has rapid exponential increase in the adsorption uptake at the start of increase in the pressure/concentration. This continues until the relative pressure reaches unity. The Type-III isotherm data is obtained from adsorbent–adsorbate pair of green coconut pulp and water as described in [41]. Based upon the proposed universal model with two probability terms, the regressed Type-III isotherms with experimental data point are shown in Figure 4, for different temperatures.
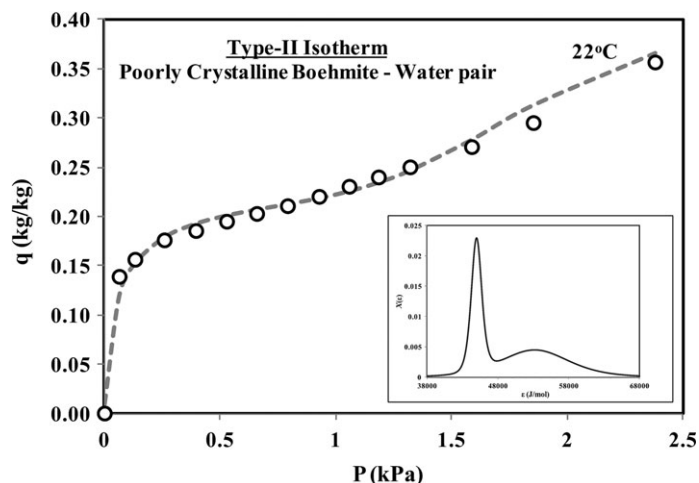

Figure 3. *Type-II adsorption isotherms experimental and prediction data.*
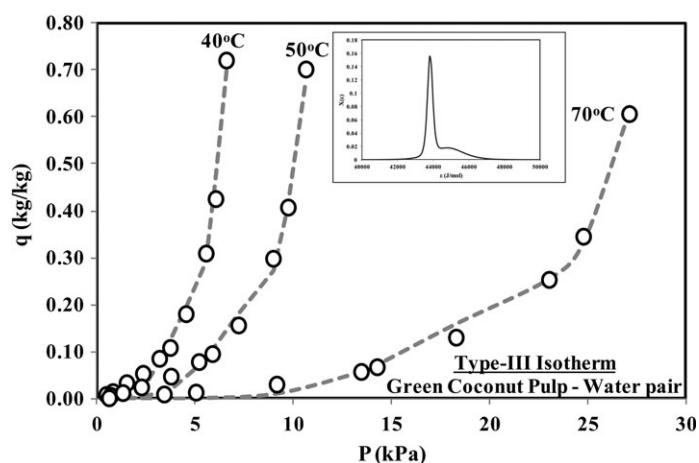

Figure 4. *Type-III adsorption isotherms experimental and prediction data.*

It can be seen that although there are two different sets of energy sites, available for different pore sizes, but the difference in their energy level is not very big. With the availability of high energy level adsorption sites, a gradual increase in the adsorption uptake can be seen with increase in the probability value of energy site.

3.4 Type-IV

The Type-IV isotherm is the combination of Type-II and Type-I isotherms. There is an intermediate saturation of adsorption surface at the low pressure/concentration. However, at higher concentration/pressure, the adsorption uptake again follows horizontal saturation, like Type-I isotherm and unlike Type-II which shows exponential increase in the uptake near saturation pressure. This kind of behavior shows the formation of multilayer adsorption. The Type-IV isotherm behavior is shown by the activated carbon and water pair [42]. The experimental data for isotherm, obtained from, and the repressed adsorption uptake obtained from proposed universal adsorption model, are shown in Figure 5. A non-symmetrical single peak energy distribution graph for Type-IV isotherm shows the multilayer formation, instead of twin peak energy distribution for different sets of pore size.

3.5 Type-V

The Type-V isotherm follows Type-III isotherm trend at low pressure/concentration, with exponential increase in the adsorption uptake. However, at higher pressure/concentration, there is gradual increase in the uptake, like Type-IV isotherm, until pressure reaches saturation. The experimental data for Type-V isotherm by Zeolite Z01 and water pair, obtained from [39], which is regressed with two term of proposed universal adsorption mode,l is shown in Figure 6. The higher uptake at lower pressure/concentration can be depicted as the larger probability of high energy adsorption sites. Like Type-III
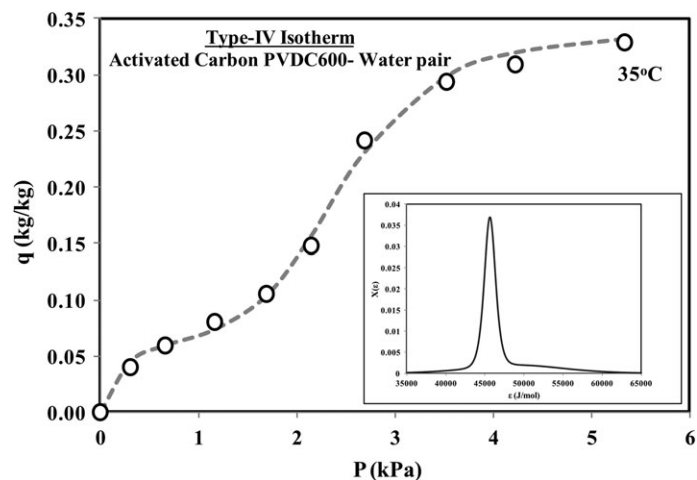

Figure 5. *Type-IV adsorption isotherms experimental and prediction data.*
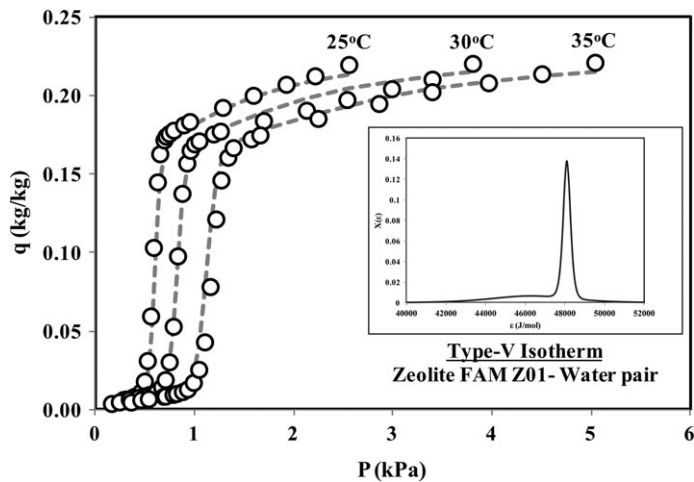
Figure 6. *Type-IV adsorption isotherms experimental and prediction data.*

isotherm, there is slight increase in the adsorption update at the start of pressure/concentration increase. After passing the peak probability adsorption energy site, there is a sharp increase in the adsorption uptake occur, which is due to larger availability of adsorption sites as seen by the adsorbate molecules to be adsorbed.

So, the proposed model theory not only describes the behavior of the isotherm against pressure/concentration, but also gives the insight of the adsorption uptake behavior against the availability of the adsorption energy site. Due to energy distribution curve, the proposed models help one to easily understand the different categories of the defined isotherm, even for adsorbent–refrigerant isotherms pairs [43–45], which also follow the described isotherm types, as the adsorption uptake clearly depends upon the availability and distribution of the adsorption energy sites.

4 CONCLUSION

Based upon the classical approach of energy distribution function and homotattic patch approximation, the proposed universal adsorption isotherm model has been presented and verified to predict the behavior of all types of the IUPAC adsorption isotherms. This is the first time that any adsorption isotherm model can capture the behavior of all isotherm types, i.e. from monolayer to multilayer formation with different pore sizes. This proposed model not only helps to predict the isotherm values, but also gives insight of the certain isotherm types by using the energy distribution curve of the adsorption energy sites. This energy distribution curve helps to understand the characteristic of certain isotherm types by giving the distribution and extent of availability of the adsorption energy site, and their effect on the rate of adsorption uptake. The proposed model is considered as a great achievement in generalizing the adsorption phenomena for all kinds of adsorbent–adsorbate

pairs, based upon the distribution and availability of adsorption energy sites over porous surface, which none of the current isotherm theories is able to define for all isotherm types. This insight analysis will help to modify or create the required porous structure, with certain adsorption surface characteristics, as per certain application requirements for specific adsorbate.

REFERENCES

[1] Burhan M, Shahzad MW, Ng KC. Long-term performance potential of concentrated photovoltaic (CPV) systems. *Energy Convers Manag* 2017;**148**:90–9.

[2] Burhan M, Shahzad MW, Ng KC. Development of performance model and optimization strategy for standalone operation of CPV-hydrogen system utilizing multi-junction solar cell. *Int J Hydrogen Energy* 2017;**42**: 26789–803.

[3] Muhammad B, Seung JO, Ng KC, *et al.* Experimental investigation of multi-junction solar cell using two axis solar tracker. *Appl Mech Mater* 2016;**819**: 536–40.

[4] Burhan M. Chua KJE, Ng KC. Simulation and development of a multi-leg homogeniser concentrating assembly for concentrated photovoltaic (CPV) system with electrical rating analysis. *Energy Convers Manag* 2016;**116**: 58–71.

[5] Burhan M, Oh SJ, Chua KJ, *et al.* Solar to hydrogen: compact and cost effective CPV field for rooftop operation and hydrogen production. *Appl Energy* 2017;**194**:255–66. doi:10.1016/j.apenergy.2016.11.062.

[6] Burhan M, Oh SJ, Chua KJE, *et al.* Double lens collimator solar feedback sensor and master slave configuration: development of compact and low cost two axis solar tracking system for CPV applications. *Sol Energy* 2016; **137**:352–63.

[7] Shahzad MW, Burhan M, Ghaffour N, *et al.* A multi evaporator desalination system operated with thermocline energy for future sustainability. *Desalination* 2017. doi:10.1016/j.desal.2017.04.013.

[8] Shahzad MW, Burhan M, Ng KC. Pushing desalination recovery to the maximum limit: membrane and thermal processes integration. *Desalination* 2017;**416**:54–64.

[9] Shahzad MW, Burhan M, Son HS, *et al.* Desalination processes evaluation at common platform: a Universal Performance Ratio (UPR) method. *Appl Therm Eng* 2018;**134**:62–7.

[10] Burhan M, Chua KJE, Ng KC. Long term hydrogen production potential of concentrated photovoltaic (CPV) system in tropical weather of Singapore. *Int J Hydrogen Energy* 2016;**41**:16729–42.

[11] Burhan M, Chua KJ, Ng KC. Sunlight to hydrogen conversion: design optimization and energy management of concentrated photovoltaic (CPV-Hydrogen) system using micro genetic algorithm. *Energy* 2016;**99**:115–28.

[12] Burhan M, Shahzad MW, Choon NK. Hydrogen at the Rooftop: compact CPV–hydrogen system to convert sunlight to hydrogen. *Appl Therm Eng* 2017;**132**:154–64.

[13] Ng KC, Burhan M, Shahzad MW, *et al.* A universal isotherm model to capture adsorption uptake and energy distribution of porous heterogeneous surface. *Sci Rep* 2017;**7**:10634.

[14] Burhan M, Chua KJE, Ng KC. Electrical rating of concentrated photovoltaic (CPV) systems: long-term performance analysis and comparison to conventional PV systems. *Int J Technol* 2016;**7**:189–96. doi:10.14716/ijtech.v7i2.2983.

[15] Rodriguez-Reinoso F, Martin-Martinez JM, Prado-Burguete C, *et al.* A standard adsorption isotherm for the characterization of activated carbons. *J Phys Chem* 1987;**91**:515–6.

[16] von Gemmingen U. The Fermi–Dirac concept for isotherms of adsorbents with heterogeneous surfaces. *Chem Eng Sci* 2005;**60**:5198–205.

[17] Tóth J. Thermodynamical correctness of gas/solid adsorption isotherm equations. *J Colloid Interface Sci* 1994;**163**:299–302.

[18] Foo KY, Hameed BH. Insights into the modeling of adsorption isotherm systems. *Chem Eng J* 2010;**156**:2–10.

[19] Marczewski AW, Jaroniec M. A new isotherm equation for single-solute adsorption from dilute solutions on energetically heterogeneous solids. *Monatsh Chem* 1983;**114**:711–5.

[20] Myers AL, Belfort G. *Fundamentals of adsorption*. Engineering Foundation, 1984.

[21] Jaroniec M, Marczewski AW. Physical adsorption of gases on energetically heterogeneous solids I. GeneralizedLangmuir equation and its energy distribution. *Monatsh Chem* 1984;**115**:997–1012.

[22] Jaroniec M, Marczewski AW. Physical adsorption of gases on energetically heterogeneous solids II. Theoretical extension of a generalized Langmuir equation and its application for analysing adsorption data. *Monatsh Chem* 1984;**115**:1013–38.

[23] Tóth J. A uniform interpretation of gas/solid adsorption. *J Colloid Interface Sci* 1981;**79**:85–95.

[24] Dubinin MM, Astakhov VA. Development of the concepts of volume filling of micropores in the adsorption of gases and vapors by microporous adsorbents. *Rus Chem Bull* 1971;**20**:13–6.

[25] Bering BP, Gordeeva VA, Dubinin MM, et al. Development of concepts of the volume filling of micropores in the adsorption of gases and vapors by microporous adsorbents. *Rus Chem Bull* 1971;**20**:17–22.

[26] Dubinin MM, Astakhov VA. Development of the concepts of volume filling of micropores in the adsorption of gases and vapors by microporous adsorbents. *Rus Chem Bull* 1971;**20**:8–12.

[27] Dubinin MM, Astakhov VA. Development of the concepts of volume filling of micropores in the adsorption of gases and vapors by microporous adsorbents. *Rus Chem Bull* 1971;**20**:3–7.

[28] Chakraborty A, Sun B. An adsorption isotherm equation for multi-types adsorption with thermodynamic correctness. *Appl Therm Eng* 2014;**72**:190–9.

[29] Khalfaoui M, Knani S, Hachicha MA, et al. New theoretical expressions for the five adsorption type isotherms classified by BET based on statistical physics treatment. *J Colloid Interface Sci* 2003;**263**:350–6.

[30] Ross S, Olivier JP. *On Physical Adsorption*. Interscience Pub., John Wiley and Sons Inc., 1964.

[31] Freundlich H. Of the adsorption of gases. Section II. Kinetics and energetics of gas adsorption. Introductory paper to section II. *T Faraday Soc* 1932;**28**:195–201.

[32] Sips R. On the structure of a catalyst surface. *J Chem Phys* 1948;**16**:490–5.

[33] Sips R. On the structure of a catalyst surface. II. *J Chem Phys* 1950;**18**:1024–6.

[34] Young DM, Crowell AD. *Physical Adsorption of Gases*. Butterworths, 1962.

[35] Jovanovic DS. Physical adsorption of gases. I. Isotherms for monolayer and multilayer adsorption. *Colloid Polym Sci* 1969;**235**:1203–13.

[36] Foo KY, Hameed BH. Insights into the modeling of adsorption isotherm systems. *Chem Eng J* 2010;**156**:2–10.

[37] Nitta T, Shigetomi T, Kuro-oka MA, et al. An adsorption isotherm of multi-site occupancy model for homogeneous surface. *J Chem Eng Jpn* 1984;**17**:39–45.

[38] Adolphs J, Setzer MJ. A model to describe adsorption isotherms. *J Colloid Interface Sci* 1996;**180**:70–6.

[39] Ang L. Experimental and theoretical studies on the heat transfer enhancement of adsorbent coated heat exchangers. *PhD thesis*. Department of Mechanical Engineering, National University of Singapore, 2014.

[40] Wang SL, Johnston CT, Bish DL, et al. Water-vapor adsorption and surface area measurement of poorly crystalline boehmite. *J Colloid Interface Sci* 2003;**260**:26–35.

[41] Lavoyer FC, Gabas AL, Oliveira WP, et al. Study of adsorption isotherms of green coconut pulp. *Food Sci Technol (Campinas)* 2013;**33**:68–74.

[42] Bansal R, Dhami T. Surface characteristics and surface behaviour of polymer carbons-II: adsorption of water vapor. *Carbon N Y* 1978;**16**:389–95.

[43] El-Sharkawy II, Kuwahara K, Saha BB, et al. Experimental investigation of activated carbon fibers/ethanol pairs for adsorption cooling system application. *Appl Therm Eng* 2006;**26**:859–65.

[44] Wang LW, Wang RZ, Oliveira RG. A review on adsorption working pairs for refrigeration. *Renew Sustain Energy Rev* 2009;**13**:518–34.

[45] Saha BB, El-Sharkawy II, Thorpe R, et al. Accurate adsorption isotherms of R134a onto activated carbons for cooling and freezing applications. *Int J Refrig* 2012;**35**:499–505.